

Light Nuclei Production in Au+Au Collisions at $\sqrt{s_{\text{NN}}} = 3, 14.6$ and 19.6 GeV from RHIC BES-II

Yixuan Jin (for the STAR collaboration)
Central China Normal University

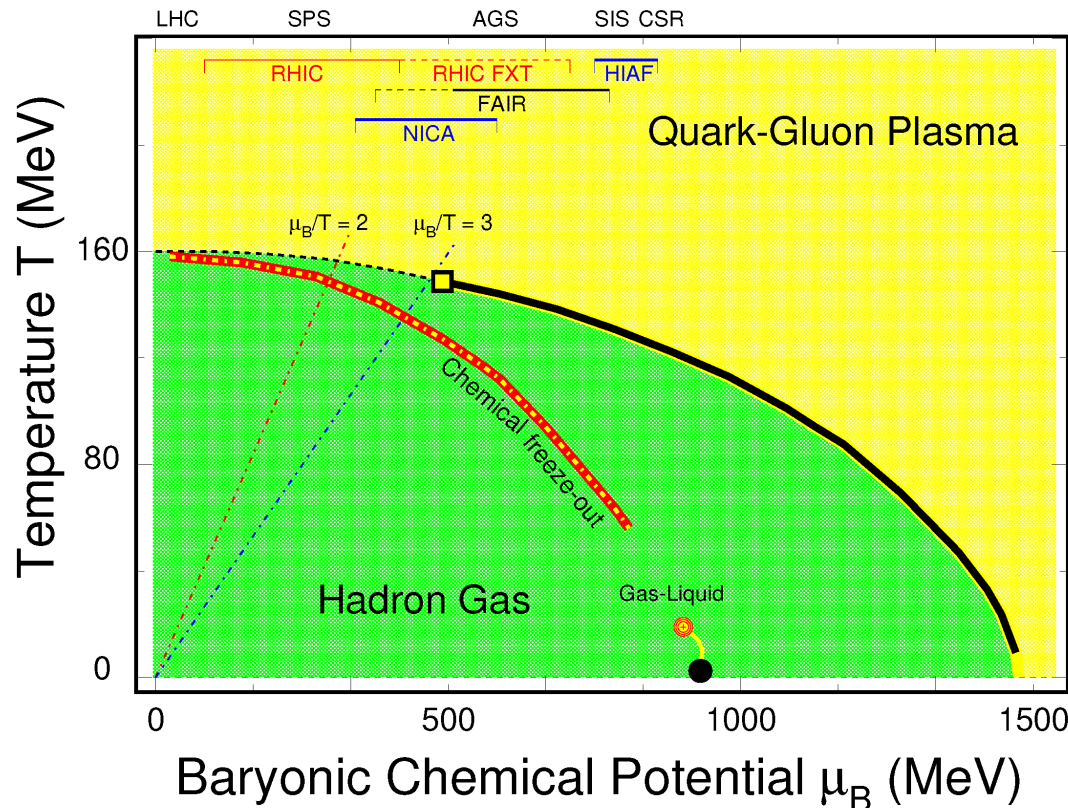
December 17, 2023



Outline

- Motivation
- The STAR Experiment
 - Dataset and Particle Identification
- Results and Discussions
 - Transverse Momentum Spectra
 - Particle Yields
 - Particle Yield Ratios
 - Coalescence Parameters
- Summary and Outlook

Motivation – QCD Phase Diagram and HIC

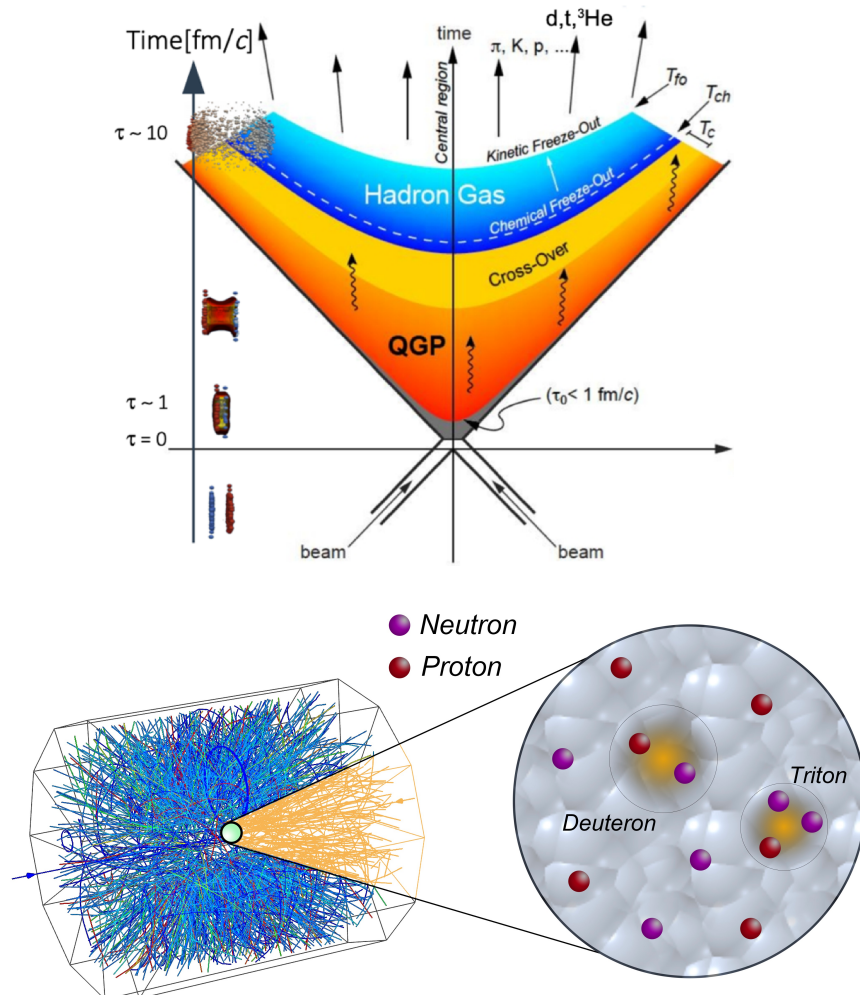


Beam Energy Scan Program at RHIC:

- ❖ Control beam energy and centrality to vary initial T and μ_B .
- ❖ Create QGP and explore its properties.
- ❖ Map out the crossover and/or 1st order QCD phase boundary.
- ❖ Search for the signatures of possible QCD critical point.

<https://drupal.star.bnl.gov/STAR/starnotes/public/sn0598>
X.F. Luo, S.S. Shi, N. Xu and Y.F. Zhang, Particles 2020, 3(2), 278-307

Motivation – Light Nuclei



K. Sun et al. Phys.Lett.B 774 (2017) 103-107
E. Shuryak et al. Phys.Rev.C 101 (2020) 3, 034914

1. Why Light Nuclei?

- ❖ Carry information about local baryon density fluctuations.
- ❖ Provide an effective probe to study 1st order phase boundary and the QCD critical point.

2. Observable : Yield ratio of light nuclei ($N_t \times N_p / N_d^2$)

- ❖ Based on coalescence model:

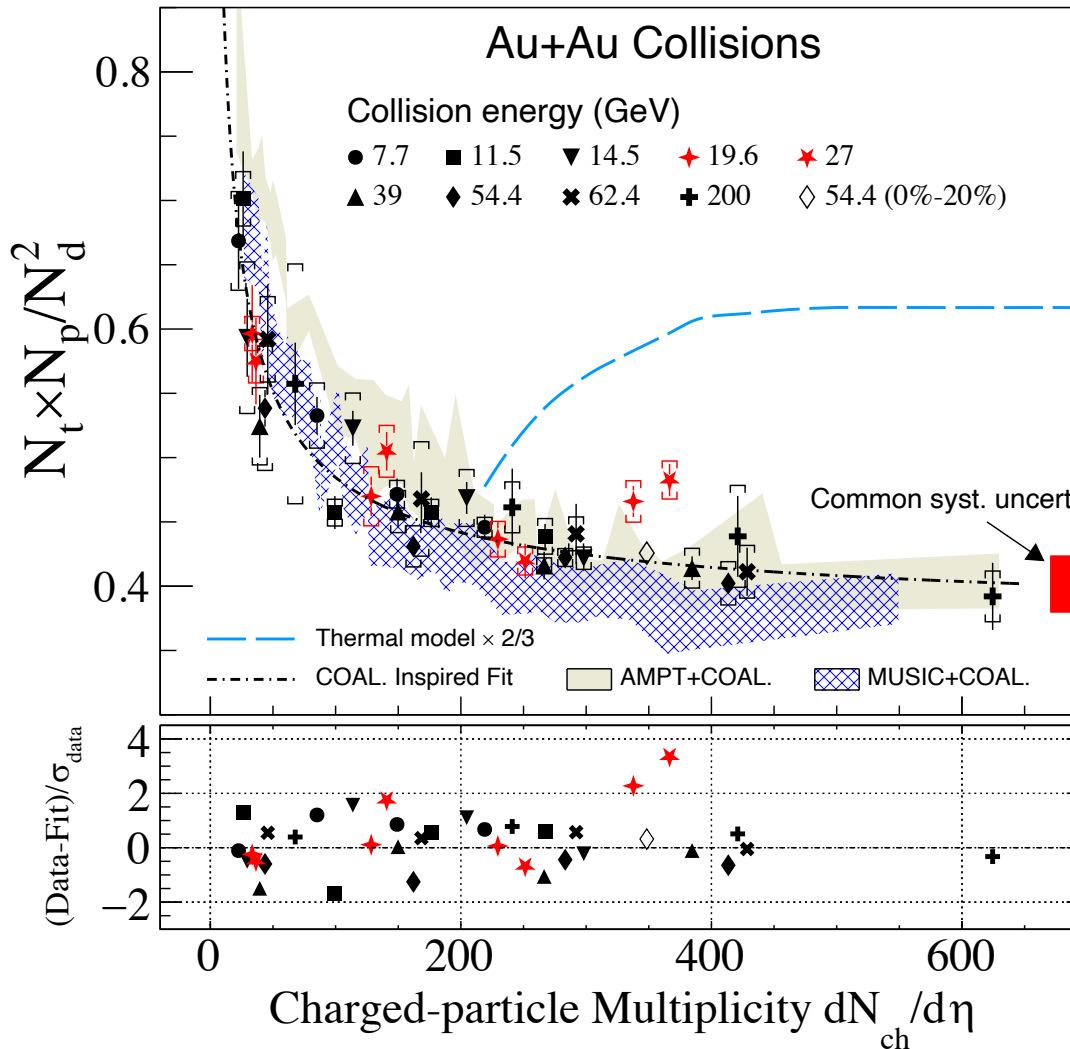
$$N_A = g_c \int d\Gamma \rho_s(\{x_i, p_i\}) \times W_A(\{x_i, p_i\})$$

- ❖ The yield ratio is related to neutron density fluctuations:

$$N_t \times N_p / N_d^2 \approx g(1 + \Delta n)$$

factor $g = \frac{1}{2\sqrt{3}}$ comes from the thermal equilibrium assumption of nucleon abundances.

Motivation – Results from RHIC BES-I

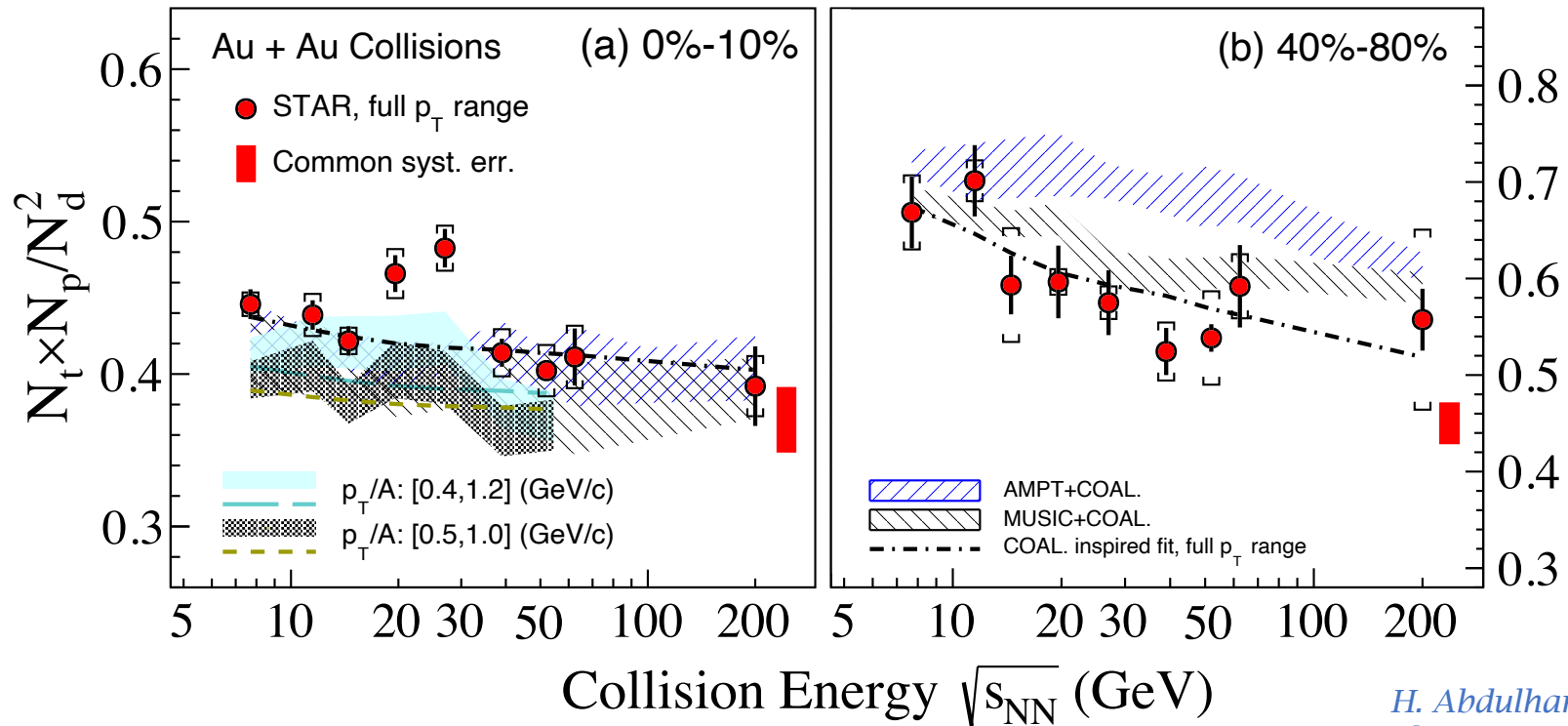


$$\frac{N_t \times N_p}{N_d} = p_0 \times \left(\frac{R^2 + \frac{2}{3} r_d^2}{R^2 + \frac{1}{2} r_t^2} \right)^3, \text{ where } R \propto (dN_{\text{ch}}/d\eta)^{1/3}.$$

- The yield ratio exhibits a scaling behavior: A trend driven by the interplay between the size of light nuclei and the size of the fireball created in HIC.
- The ratio of 19.6 and 27 GeV from 0-10% centrality show enhancements with respect to the coalescence baseline with a combined significance of 4.1σ .
- The thermal model overestimates the experimental data and shows a clear difference compared to the coalescence model.

H. Abdulhamid et al. [STAR Collaboration] Phys. Rev. Lett 130, 202301 (2023)
W. Zhao, K. J. Sun, C. M. Ko and X. Luo, Phys. Lett. B 820, 136571 (2021)

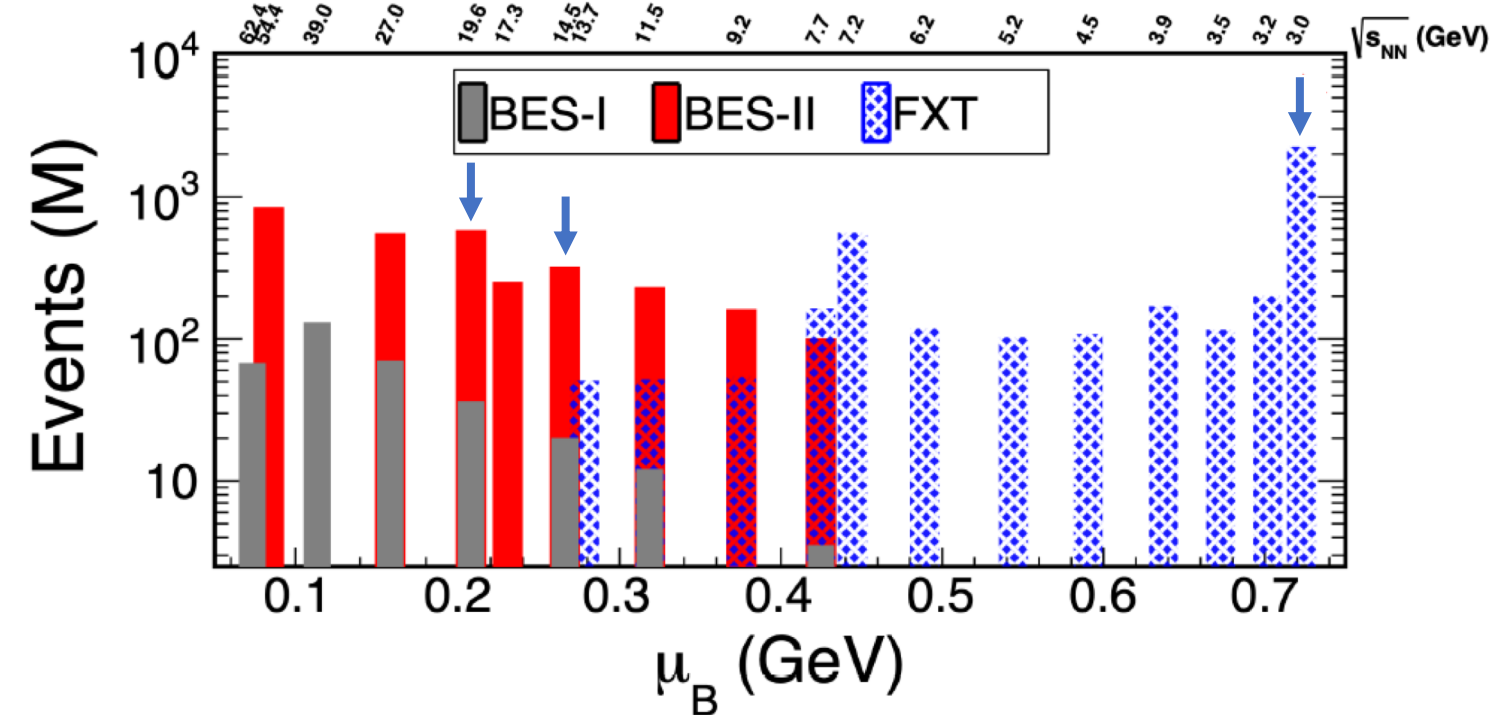
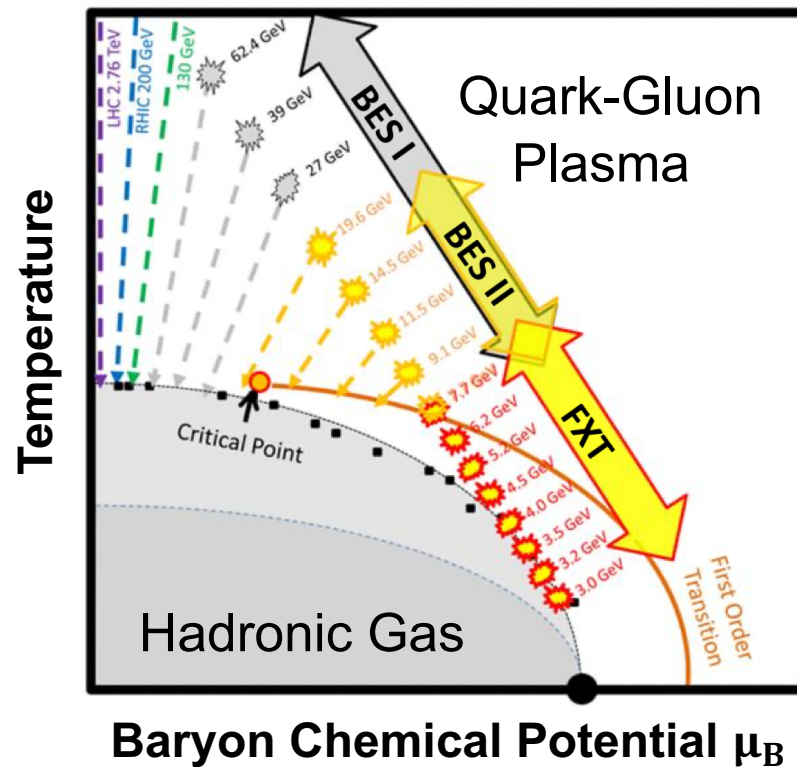
Motivation – Results from RHIC BES-I



H. Abdulhamid et al. [STAR Collaboration]
Phys. Rev. Lett 130, 202301 (2023)

- **Non-monotonic** behavior observed in 0-10% central Au+Au collisions around 19.6 and 27 GeV.
- **Monotonic behavior** in peripheral collisions, and can be well described by coalescence models.
- Flat trends are predicted by theoretical models of AMPT and MUSIC + UrQMD hybrid model.

RHIC Beam Energy Scan Program

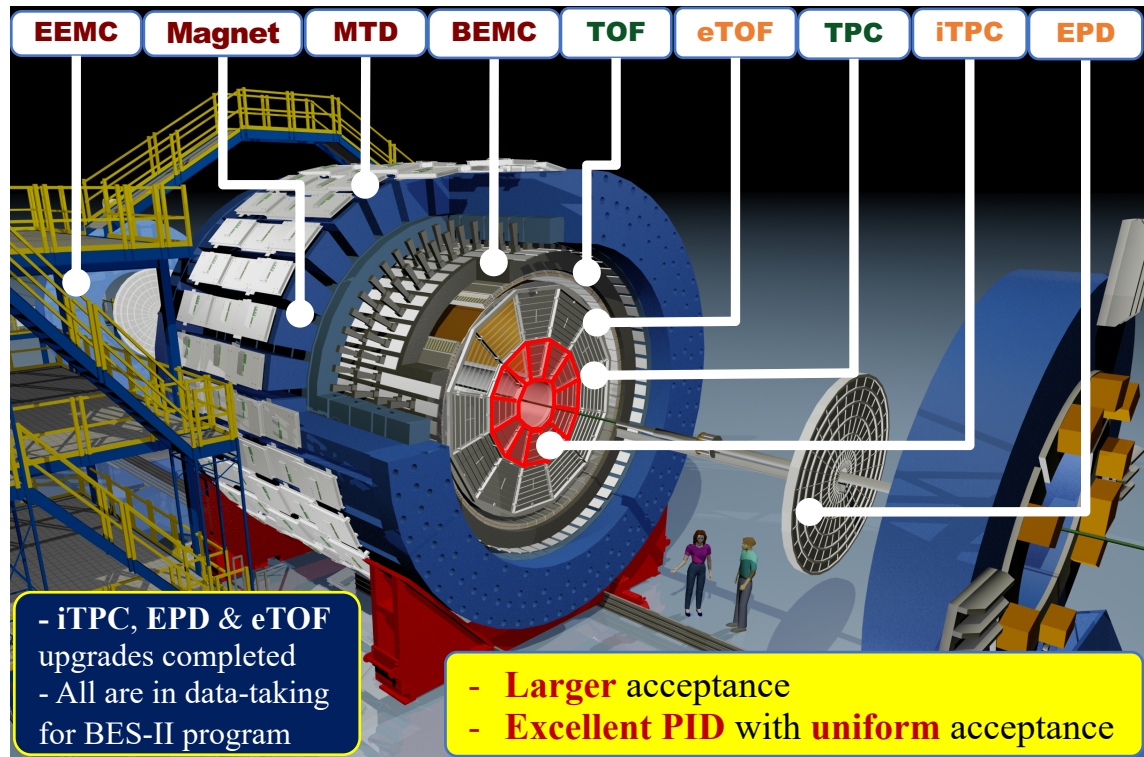


- ❖ STAR has completed BES-II data-taking with factors of 10 – 20 more statistics compared to BES-I.
- ❖ BES-II: 8 collider energies (7.7 – 54 GeV) / 12 FXT energies (3.0 – 13.7 GeV)
- ❖ μ_B coverage : $25 < \mu_B < 750$ MeV.

STAR, arXiv:1007.2613
<https://drupal.star.bnl.gov/STAR/starnotes/public/sn0493>
<https://drupal.star.bnl.gov/STAR/starnotes/public/sn0598>

The Solenoidal Tracker At RHIC (STAR)

Detector upgrades for STAR BES-II



iTPC:

- Improves dE/dx
- Extends η coverage from 1.0 to 1.5
- Lower p_T cut-in from 125 to 60 MeV/c
- Ready in 2019

eTOF:

- Forward rapidity coverage
- η coverage from 0.9 to 1.5
- Borrowed from CBM-FAIR
- Ready in 2019

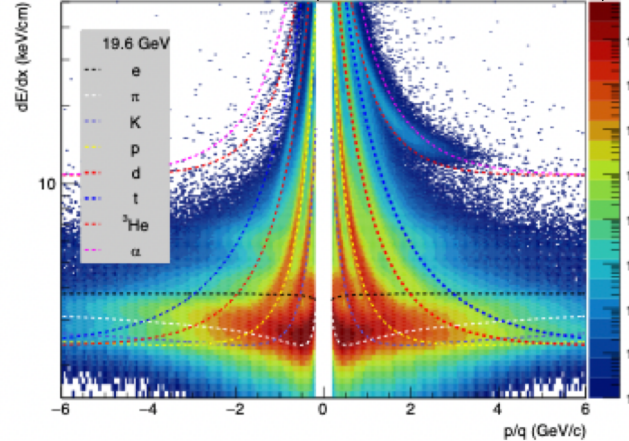
iTPC: <https://drupal.star.bnl.gov/STAR/starnotes/public/sn0619>

eTOF: [STAR and CBM eTOF group, arXiv: 1609.05102](#)

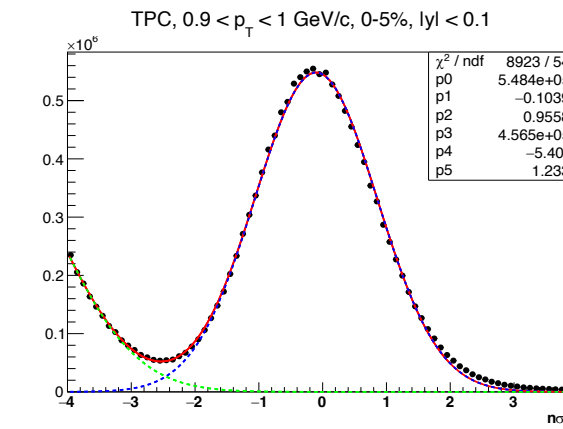
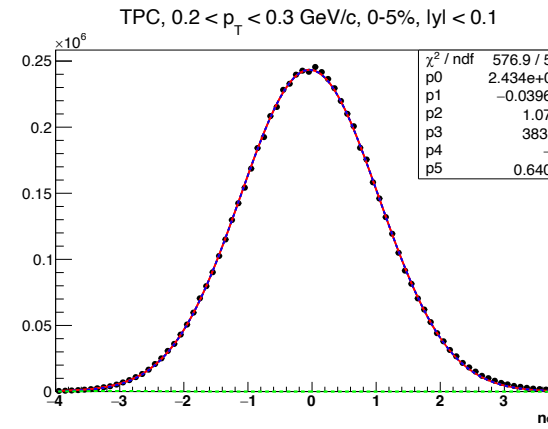
- ❖ Enlarge rapidity acceptance
- ❖ Improve particle identification

Particle Identification and Signal Extraction

$$\text{TPC: } z = \log\left(\frac{\langle dE/dx \rangle_{\text{measure}}}{\langle dE/dx \rangle_{\text{Bichsel}}}\right)$$



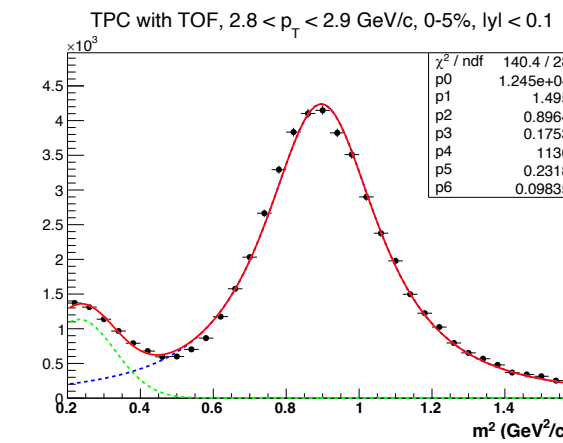
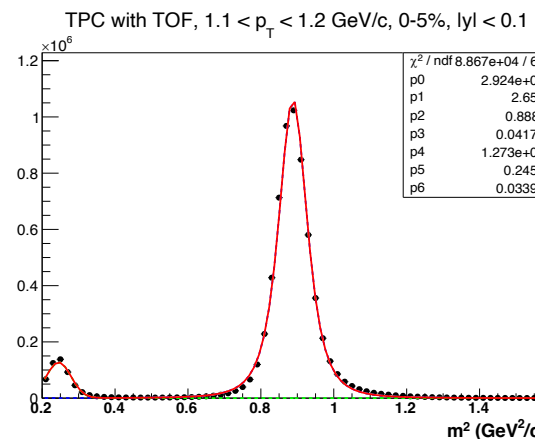
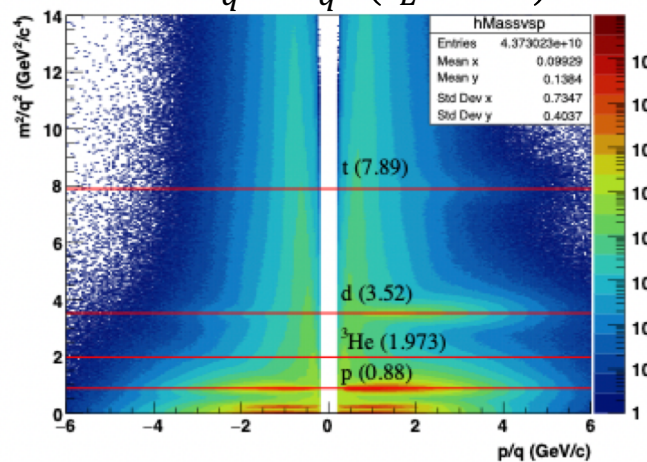
Signal Extraction Examples (19.6 GeV, proton, 0-5%)



Low p_T : TPC

Signal: Gaussian (Blue)
 BG: Gaussian (Green)
 Total: (Red)

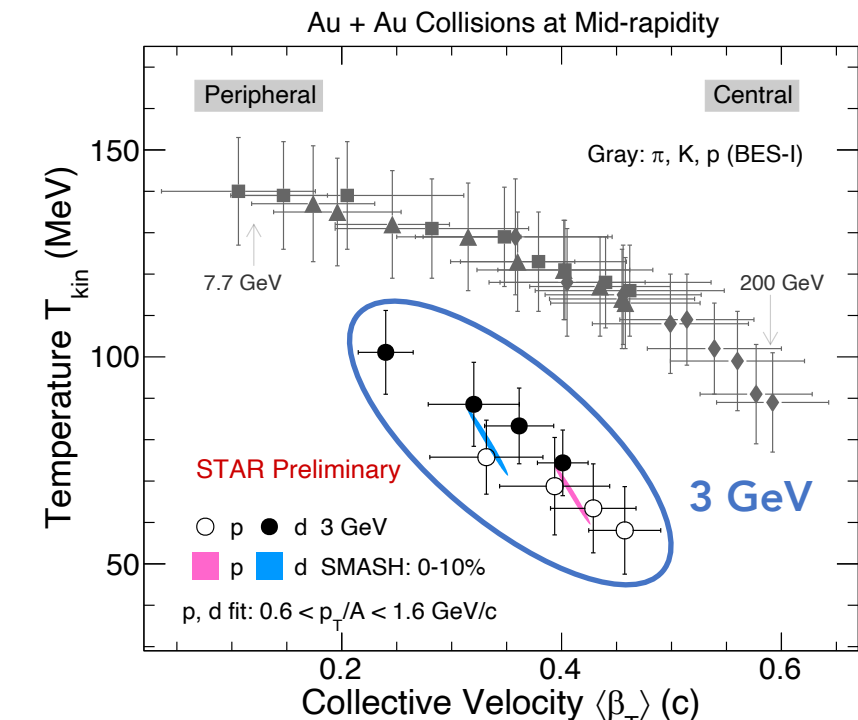
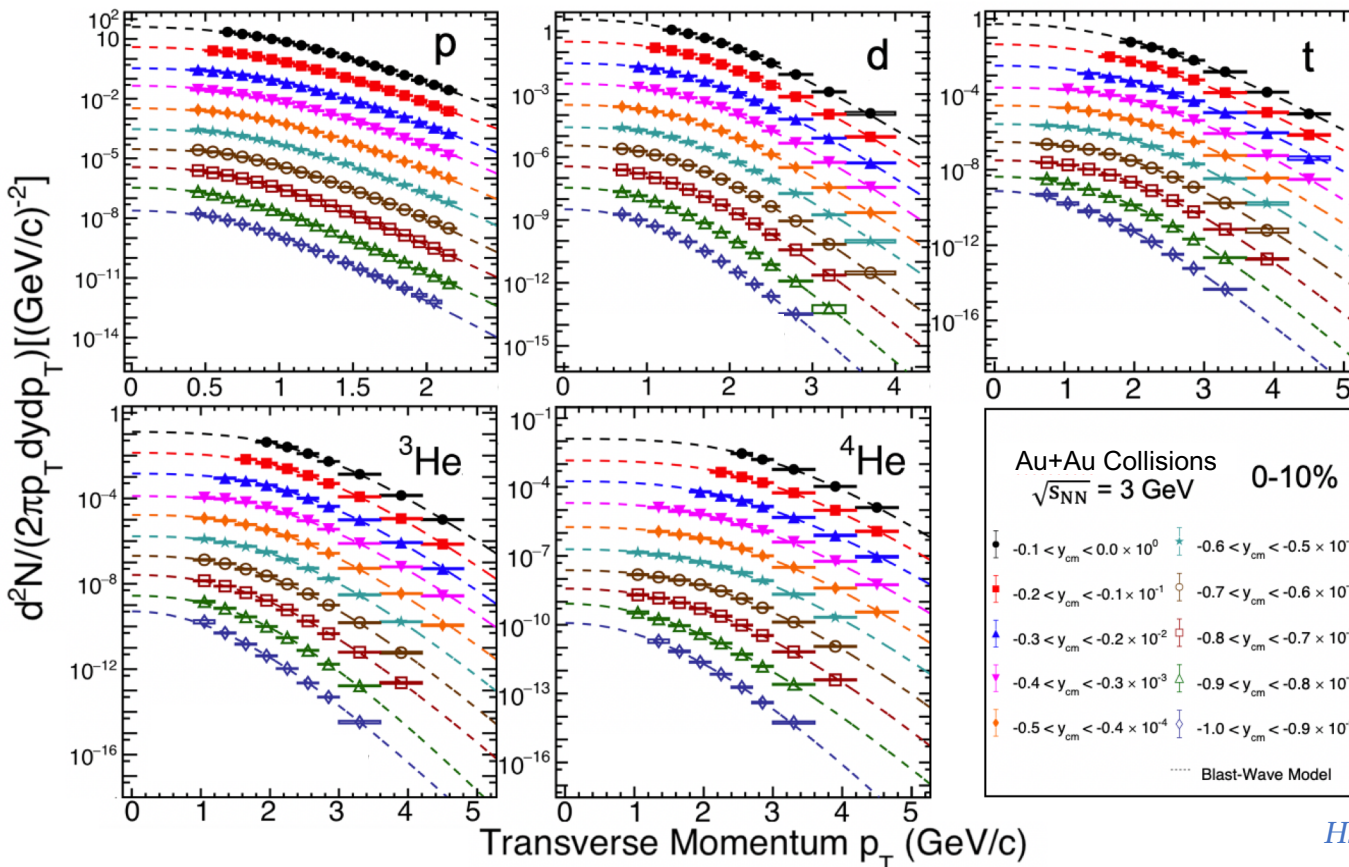
$$\text{TOF: } \frac{m^2}{q^2} = \frac{p^2}{q^2} \left(\frac{c^2 t^2}{L^2} - 1 \right)$$



High p_T : TPC with TOF

Signal: Student-t (Blue)
 BG: Gaussian (Green)
 Total: (Red)

Results from RHIC FXT at $\sqrt{s_{NN}} = 3 \text{ GeV}$



H. Liu. [STAR Collaboration] Acta Phys. Polon. Supp. 16, 1-A148 (2023)

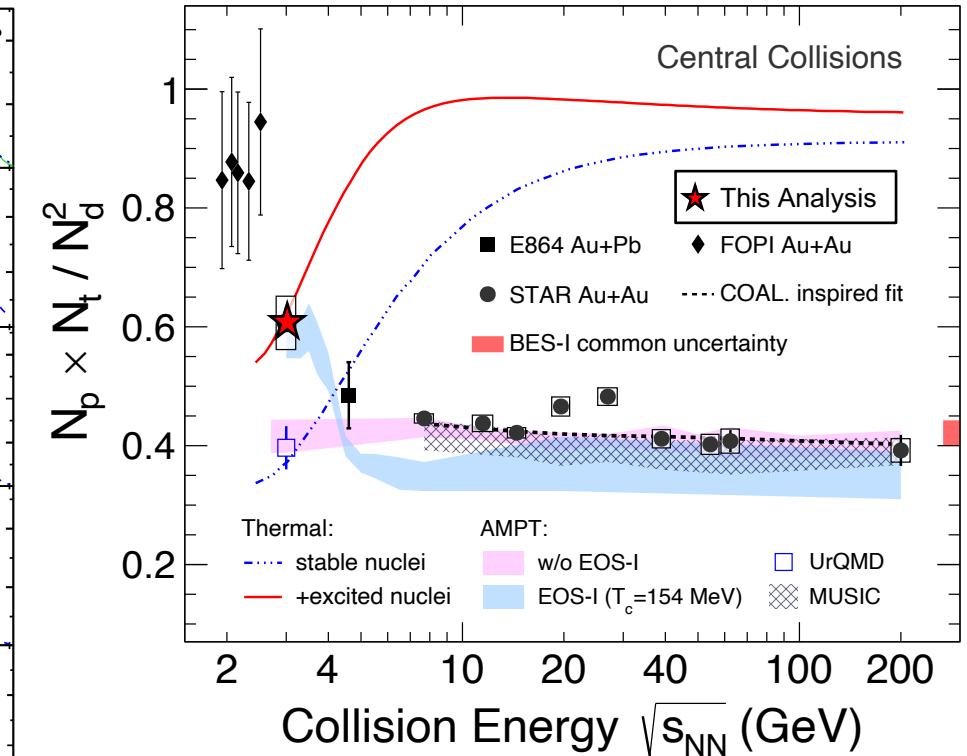
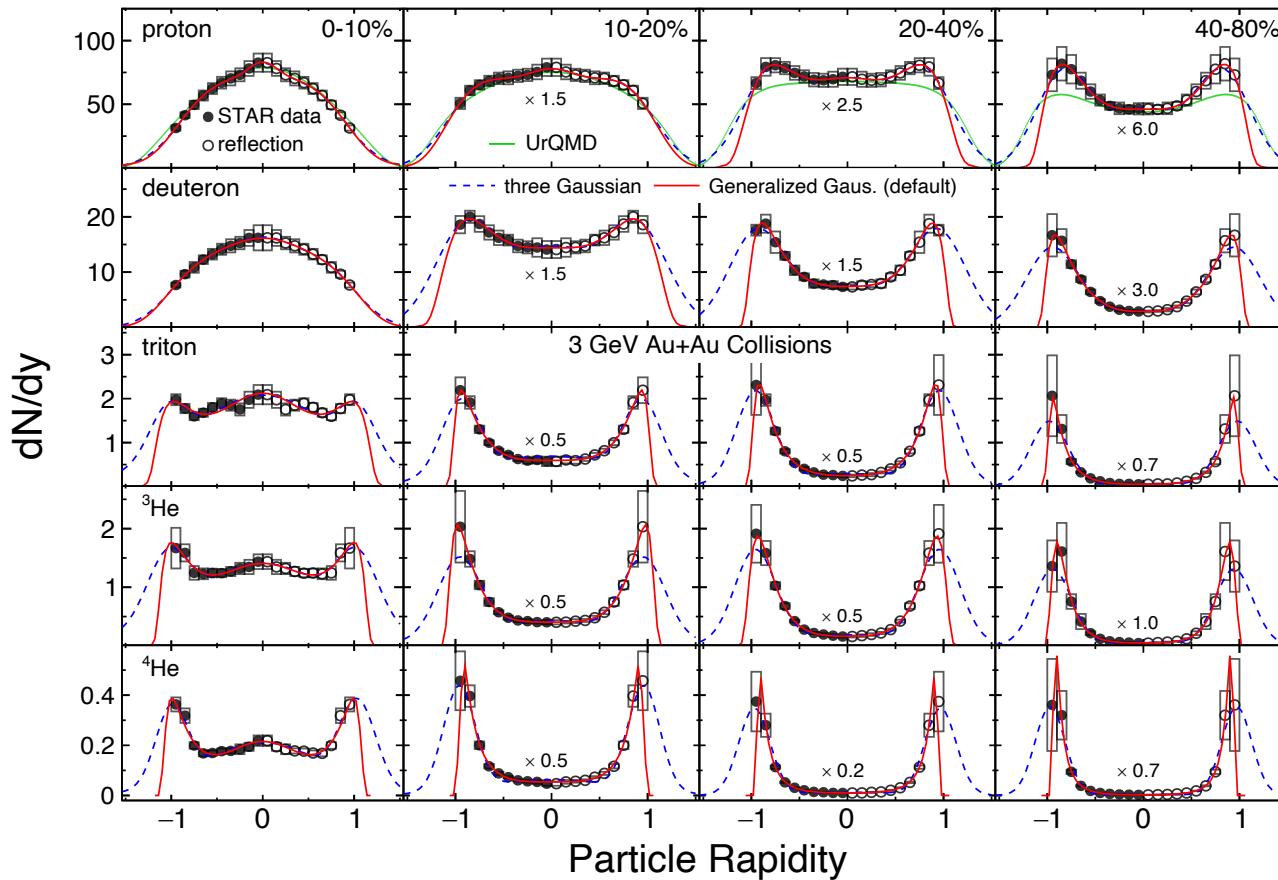
- The first measurement of light nuclei production (p, d, t, ${}^3\text{He}$, ${}^4\text{He}$) in Au + Au collisions at $\sqrt{s_{NN}} = 3 \text{ GeV}$ from STAR experiment.
- At 3 GeV Au+Au collisions, the kinetic freeze-out parameters (T_{kin} , $\langle \beta_T \rangle$) show different trend compared to that of higher energy collisions.
- The freeze-out parameter (T_{kin}) of deuteron is systematically higher than that of proton at 3 GeV, which is different from higher energies.



Indicate a different equation of state (EoS)

Similar trend seen in SMASH Model
 $T_{\text{kin}}^d > T_{\text{kin}}^p$

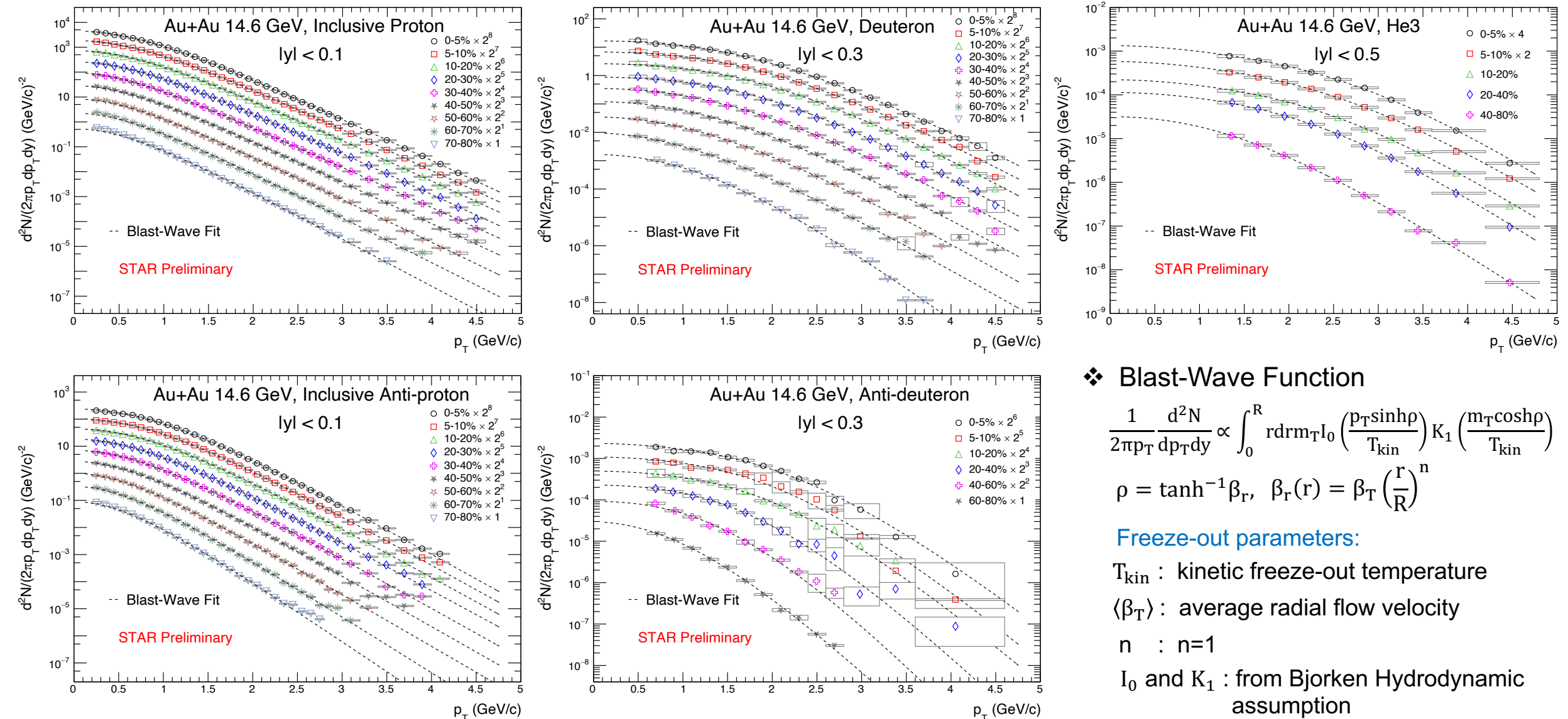
Results from RHIC FXT at $\sqrt{s_{NN}} = 3 \text{ GeV}$



STAR, arXiv: 2311.11020

- Measured the rapidity dependence of light nuclei production.
 - The centrality dependence of rapidity density is attributed to the interplay between baryon stopping and the spectators' contribution.
- The yield ratio $N_t \times N_p / N_d^2$ of mid-rapidity measured at 3 GeV follow the trend of world data.

Transverse Momentum Spectra at 14.6 GeV



❖ Blast-Wave Function

$$\frac{1}{2\pi p_T} \frac{d^2N}{dp_T dy} \propto \int_0^R r dr m_T I_0 \left(\frac{p_T \sinh \rho}{T_{kin}} \right) K_1 \left(\frac{m_T \cosh \rho}{T_{kin}} \right)$$

$$\rho = \tanh^{-1} \beta_r, \quad \beta_r(r) = \beta_T \left(\frac{r}{R} \right)^n$$

Freeze-out parameters:

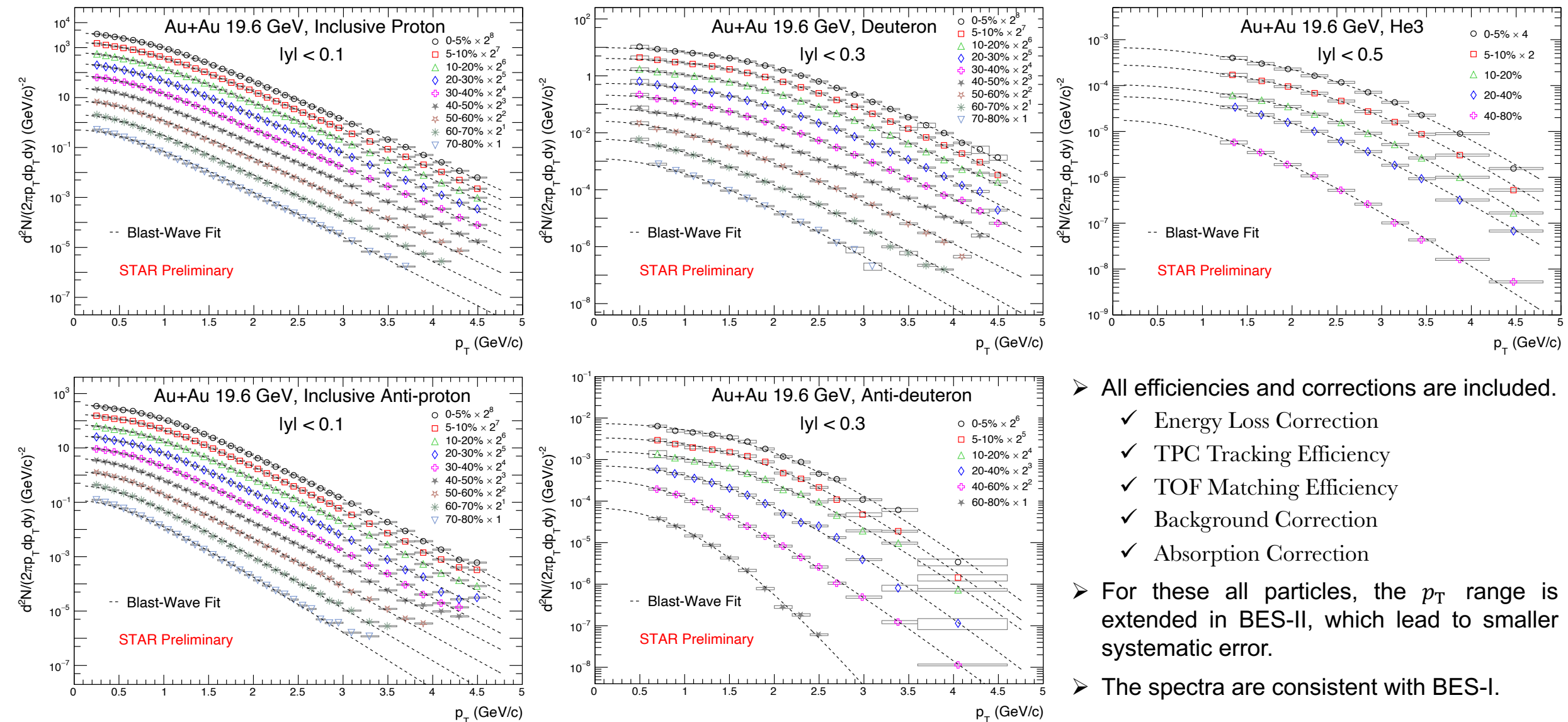
T_{kin} : kinetic freeze-out temperature

$\langle \beta_T \rangle$: average radial flow velocity

n : $n=1$

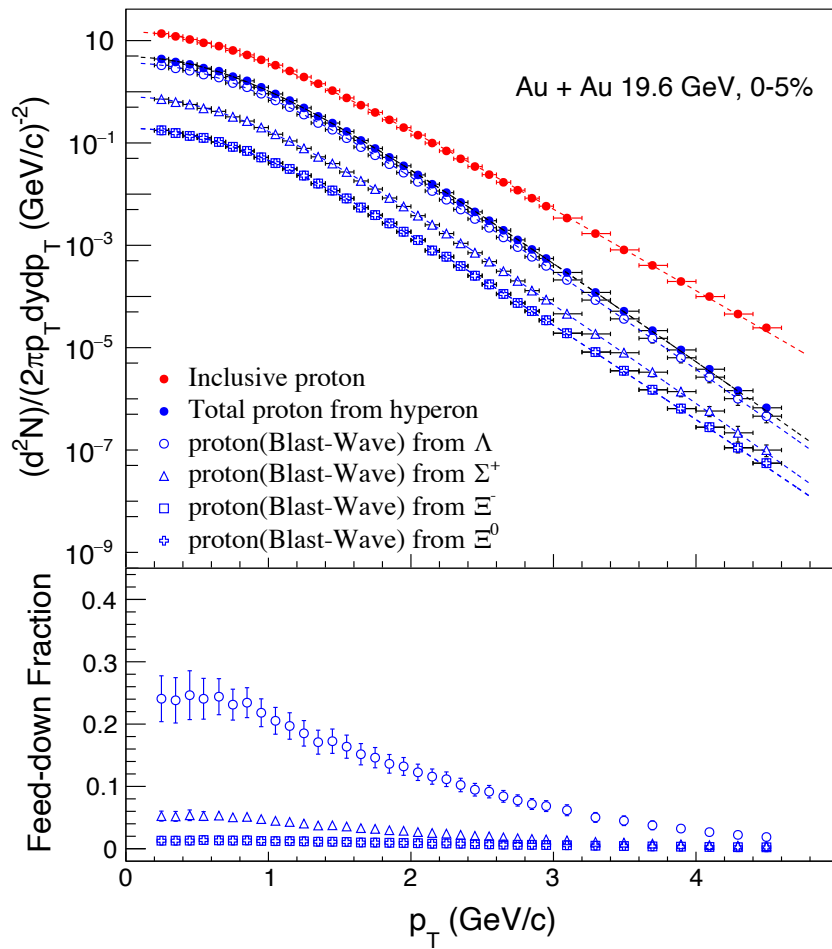
I_0 and K_1 : from Bjorken Hydrodynamic assumption

Transverse Momentum Spectra at 19.6 GeV

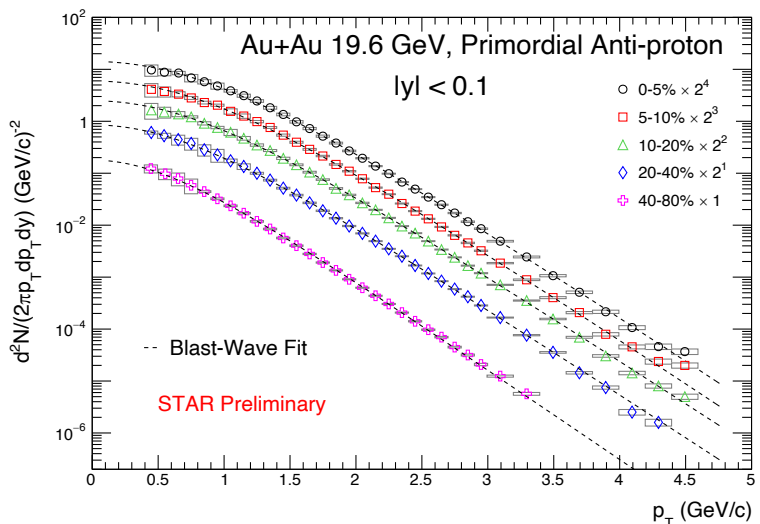
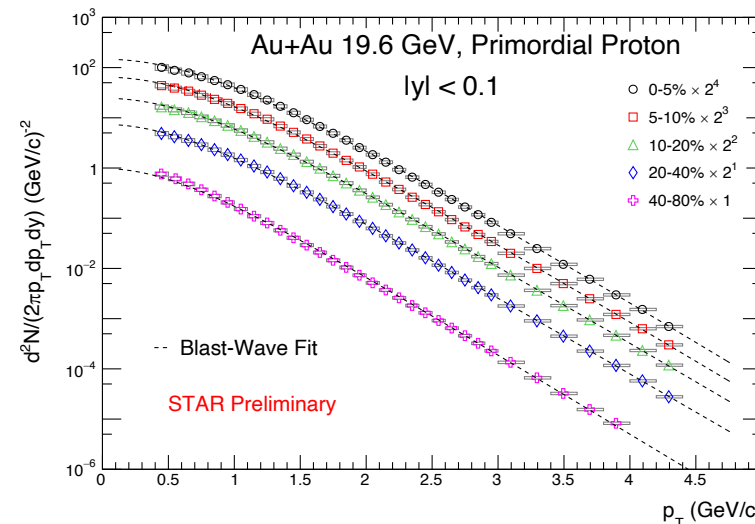


- All efficiencies and corrections are included.
 - ✓ Energy Loss Correction
 - ✓ TPC Tracking Efficiency
 - ✓ TOF Matching Efficiency
 - ✓ Background Correction
 - ✓ Absorption Correction
- For these all particles, the p_T range is extended in BES-II, which lead to smaller systematic error.
- The spectra are consistent with BES-I.

Proton Weak Decay Feed-down Correction

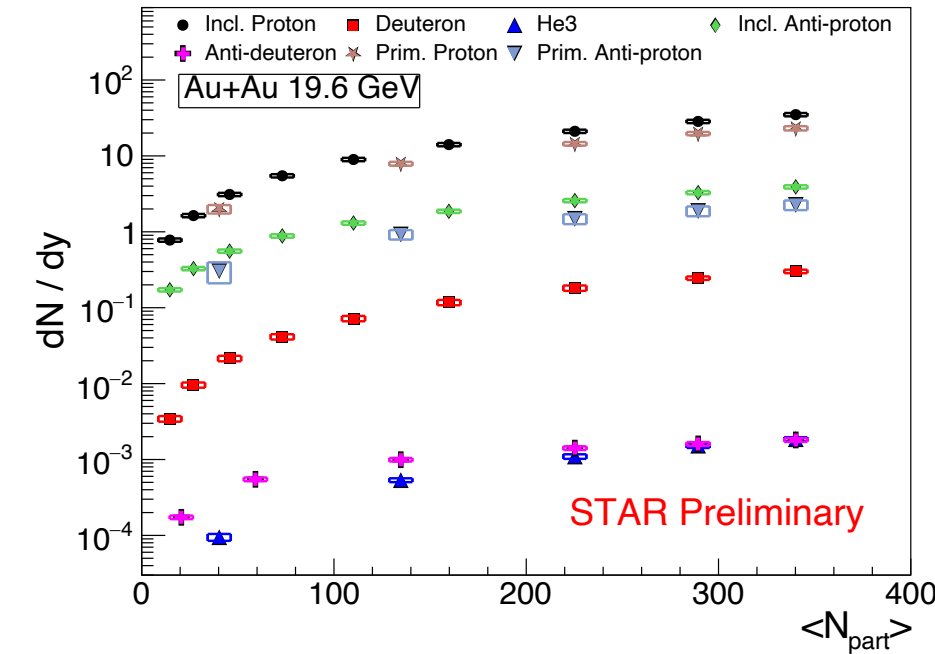
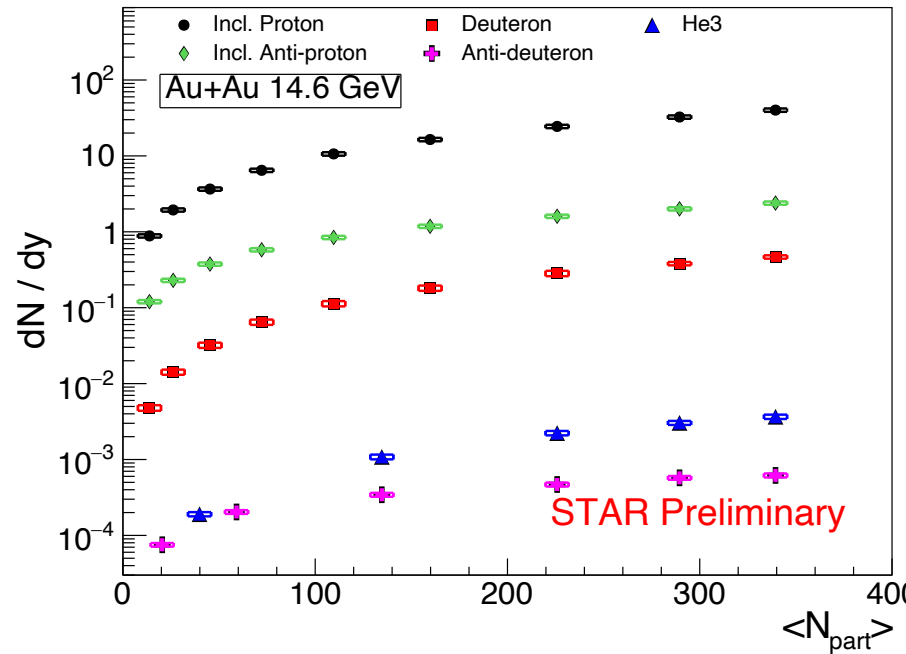


$\Lambda \rightarrow p + \pi^-$, branching ratio = 63.9 %
 $\Sigma^+ \rightarrow p + \pi^0$, branching ratio = 51.57 %
 $\Xi^- \rightarrow \Lambda + \pi^-$, branching ratio = 99.887 %
 $\Xi^0 \rightarrow \Lambda + \pi^0$, branching ratio = 99.524 %



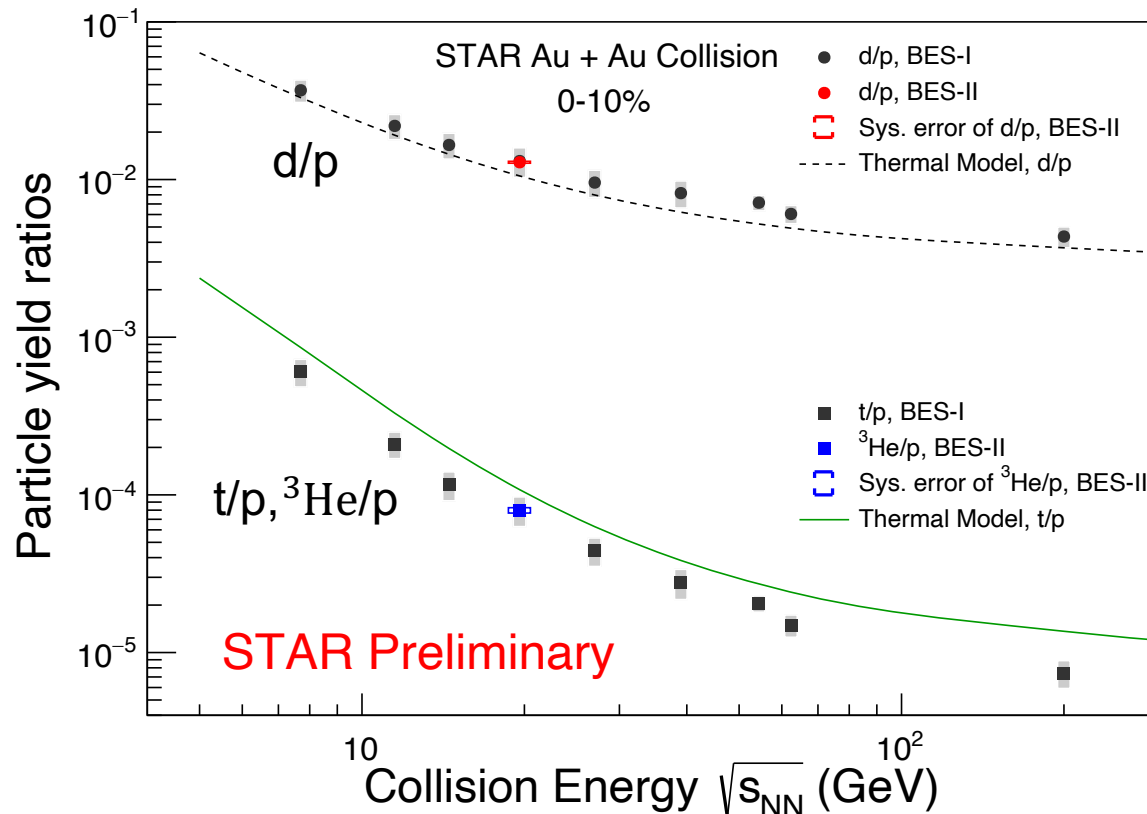
- The primordial spectra were obtained by subtracting the proton/anti-proton weak decayed from strange hadrons.
- Data driven method:
Use STAR published strange particle ($\Lambda, \Sigma^+, \Xi^-, \Xi^0$) yield and embedding simulation samples.
- The spectra of Σ^+ were obtained by multiplying the Λ spectra by a factor of 0.27.
- The spectra of Ξ^0 were assumed the same as Ξ^- .

Centrality Dependence of dN/dy



- Yields for light nuclei increase from peripheral to central collisions.
- dN/dy for positive particle decrease with increasing energy, while antiparticles are the opposite.
 - Light nuclei production is as a result of an interplay between baryon stopping and pair production.
 - The baryon stopping effect lead to high baryon density at mid-rapidity.

Particle Ratios



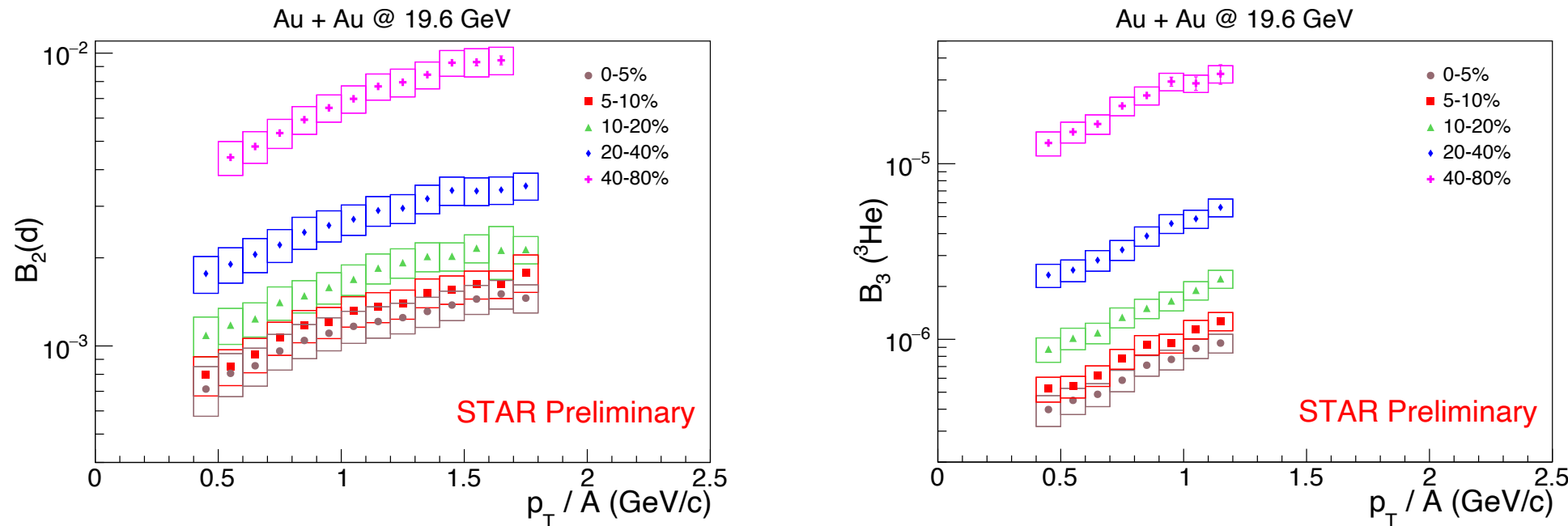
- The particle ratios show a monotonic decrease with collision energy.
- d/p ratio can be described well by the thermal model.
- The thermal model overestimates t/p and ${}^3\text{He}/p$ by a factor of approximately two.
 - The hadronic re-scatterings may play a crucial role during the hadronic expansion phase which lead to this discrepancy.

V. Vovchenko, B. Do\u0107igus, B. Kardan, M. Lorenz, and H. Stoecker,
Phys. Lett. B, 135746 (2020);

K.J. Sun, R. Wang, C. M. Ko, Y.G. Ma, and C. Shen,
arXiv: 2207.12532, (2022);

H. Abdulhamid et al. [STAR Collaboration]
Phys. Rev. Lett 130 (2023)

Coalescence Parameters



- ❖ In the coalescence picture, the invariant yield of light nuclei is proportional to the invariant yield of nucleons. The coalescence parameter B_A reflects the probability of nucleon coalescence, which is related to the local nucleon density.

$$E_A \frac{d^3 N_A}{d^3 p_A} = B_A \left(E_p \frac{d^3 N_p}{d^3 p_p} \right)^Z \left(E_n \frac{d^3 N_n}{d^3 p_n} \right)^{A-Z} \approx B_A \left(E_p \frac{d^3 N_p}{d^3 p_p} \right)^A .$$

*R. Scheibl and U. Heinz Phys.Rev.C 59 (1999) 1585-1602
J. Adam et al. [STAR Collaboration] Phys.Rev.C 99 (2019) 6, 064905*

- B_A increase with increasing p_T which might indicate an expanding collision system.
- B_A increase from central to peripheral collisions, which can be explained by a decreasing source volume.

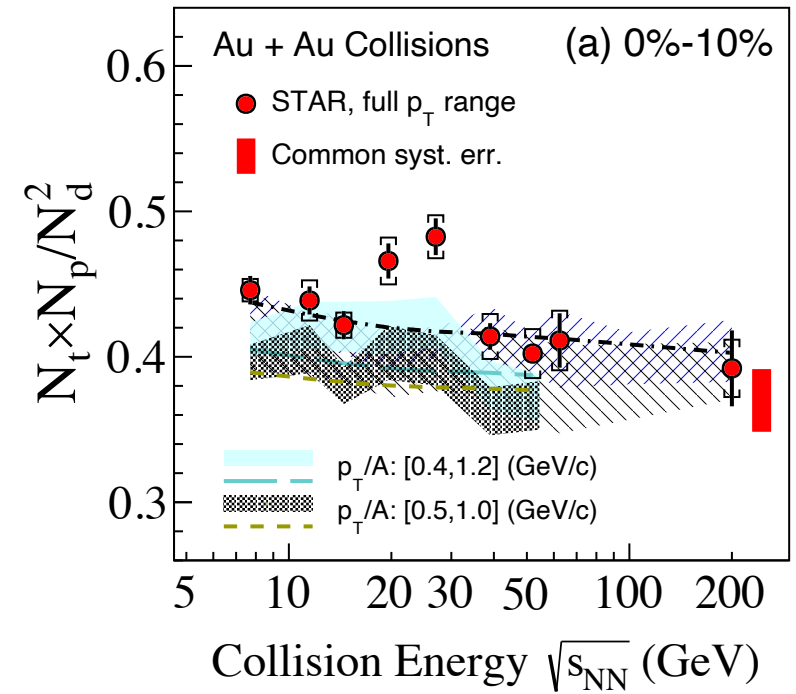
Summary and Outlook

Summary:

- We report the light nuclei productions in Au+Au collisions from RHIC STAR BES-II.
 - The centrality and rapidity dependences for p, d, t, ^3He and ^4He at 3 GeV.
 - The centrality dependence of p, d, ^3He , \bar{p} and \bar{d} at 14.6 and 19.6 GeV.
- The particle ratios N_d/N_p and $N_{^3\text{He}}/N_p$ have been measured for Au+Au collisions at 19.6 GeV in BES-II.
 - The particle ratios show a monotonic decrease with collision energy.
 - The thermal model over-predicts t/p and $^3\text{He}/p$ by a factor of about 2.
- Due to collective expansion, coalescence parameter B_A is found to increase from central to peripheral collisions and from low to high p_T .

Outlook:

- ❖ Working on other BES-II energies.



Thank you for your attention!

Back Up

| Au+Au collisions at RHIC (Collider mode) | | | | Au+Au collisions at RHIC (Fixed-Target) | | | | |
|--|-------------|---------------|------------|---|------------------|-------------|---------------|----------------|
| $\sqrt{s_{NN}}$ (GeV) | nEvents (M) | μ_B (MeV) | Time | $\sqrt{s_{NN}}$ (GeV) | E_{beam} (GeV) | nEvents (M) | μ_B (MeV) | Time |
| 200 | 380 | 25 | Run-10, 19 | 13.7 | 100 | 50 | 280 | Run-21 |
| 62.4 | 46 | 75 | Run-10 | 11.5 | 70 | 50 | 320 | Run-21 |
| 54.4 | 1200 | 85 | Run-17 | 9.2 | 44.5 | 50 | 370 | Run-21 |
| 39 | 86 | 112 | Run-10 | 7.7 | 31.2 | 260 | 420 | Run-18, 19, 20 |
| 27 | 585 | 156 | Run-11, 18 | 7.2 | 26.5 | 470 | 440 | Run-18, 20 |
| 19.6 | 595 | 206 | Run-11, 19 | 6.2 | 19.5 | 120 | 490 | Run-20 |
| 17.3 | 256 | 230 | Run-21 | 5.2 | 13.5 | 100 | 540 | Run-20 |
| 14.6 | 340 | 262 | Run-14, 19 | 4.5 | 9.8 | 110 | 590 | Run-20 |
| 11.5 | 57 | 316 | Run-10, 20 | 3.9 | 7.3 | 120 | 633 | Run-20 |
| 9.2 | 160 | 372 | Run-20 | 3.5 | 5.75 | 120 | 670 | Run-20 |
| 7.7 | 104 | 420 | Run-10, 21 | 3.2 | 4.59 | 200 | 699 | Run-19 |
| | | | | 3.0 | 3.85 | 2300 | 750 | Run-18, 21 |

- ❖ STAR has completed BES-II data-taking with factors of 10-20 more statistics compared to BES-I.
- ❖ BES-II: 8 collider energies (7.7 – 54 GeV) / 12 FXT energies (3.0 - 13.7 GeV)
- ❖ μ_B coverage : $25 < \mu_B < 750$ MeV.

STAR, arXiv:1007.2613
<https://drupal.star.bnl.gov/STAR/starnotes/public/sn0493>
<https://drupal.star.bnl.gov/STAR/starnotes/public/sn0598>